



# Late Pleistocene to Holocene vegetation dynamics in northern Kamchatka (northeastern Russia) inferred from pollen records

Valerii E. Pimenov<sup>1,\*</sup>, Maria M. Pevzner<sup>2</sup>, Timur D. Karimov<sup>3</sup>,  
Roman I. Nechushkin<sup>2</sup>, Anton V. Poleshchuk<sup>2</sup> & Dariya M. Nekrasova<sup>1</sup>

Valerii E. Pimenov<sup>1</sup>  
e-mail: v-pimenov01@inbox.ru

Maria M. Pevzner<sup>2</sup>  
e-mail: m\_pevzner@mail.ru

Timur D. Karimov<sup>3</sup>  
e-mail: karimovt@mail.ru

Roman I. Nechushkin<sup>2</sup>  
e-mail: nechrom@yandex.ru

Anton V. Poleshchuk<sup>2</sup>  
e-mail: anton302@mail.ru

Dariya M. Nekrasova<sup>1</sup>  
e-mail: dasha.nekrasova.04@mail.ru

<sup>1</sup> Faculty of Biology, Lomonosov Moscow State University, Moscow, Russia

<sup>2</sup> Geological Institute RAS, Moscow, Russia

<sup>3</sup> D-REAMS Laboratory, Weizmann Institute of Science, Rehovot, Israel

\* corresponding author

Manuscript received: 20.06.2025

Review completed: 31.08.2025

Accepted for publication: 10.09.2025

Published online: 12.09.2025

## ABSTRACT

Northern Kamchatka represents one of the most understudied regions of Beringia in paleoecological research. To reconstruct vegetation dynamics, we analyzed a peat core from Hadey mire using pollen analysis, tephrostratigraphy, and radiocarbon dating. Our results indicate peat initiation at 12.7 kyr BP, followed by a 2.5 kyr hiatus due to deposition of the Ozernovsky tephra at 12.6 kyr BP. Two pronounced decreases in peat accumulation rates correlate with warm-dry periods across the peninsula. Late Pleistocene pollen assemblages record alder shrublands and meadow-tundra vegetation indicative of cold climate. Birch forests became dominant after 4 kyr BP, whereas the establishment of dwarf pine communities occurred later, around 2 ka BP. Regional comparisons suggest a south-to-north migration pattern for birch forests whereas the expansion of dwarf pine occurred from two primary centers: the central part of the Sredinny Range and the Koryak Mountains.

**Keywords:** vegetation reconstruction, pollen analysis, tephra, volcanos, north Kamchatka, peat sediments, Pleistocene, Holocene

## РЕЗЮМЕ

**Пименов В.Е., Певзнер М.М., Каримов Т.Д., Нечушкин Р.И., Полещук А.В., Некрасова Д.М. Динамика растительности северной Камчатки (северо-восток России) в позднем плейстоцене и голоцене по данным спорово-пыльцевого анализа.** Северная Камчатка представляет собой один из самых малоизученных регионов Западной Берингии в контексте палеоэкологических исследований. Для реконструкции динамики растительности мы проанализировали торфяные отложения верхового болота Хадей применив методы спорово-пыльцевого анализа, тephростратиграфии и радиоуглеродного датирования. Торфообразование началось 12,7 тыс. л.н., однако выпадение тephры Озерновского потока (12,6 тыс. л.н.) привело к перерыву торфообразования в 2,5 тыс. лет. По данным модели возраст-глубина периоды снижения скорости осадконакопления соответствовали периодам более теплого и сухого климата в голоцене. Результаты пыльцевого анализа демонстрируют доминирование сообществ ольхового стланика и тундровых ценозов в позднем плейстоцене, что свидетельствует о холодном климате. Березовые леса стали доминировать на изучаемой территории лишь 4 тыс. л.н., в то время как распространение кедрового стланика произошло позже, около 2 тыс. л.н. Сопоставление полученных данных и региональных реконструкций позволило реконструировать пути распространения березовых лесов с юга на север полуострова, в то время как кедровый стланик имел два центра расселения: центральная часть Срединного хребта и Корьякское нагорье.

**Ключевые слова:** реконструкция растительности, пыльцевой анализ, тephра, вулканы, северная Камчатка, торфяные отложения, плейстоцен, голоцен

Tephrostratigraphic analysis is a crucial component of comprehensive paleoecological studies in volcanically active regions, such as the Kamchatka Peninsula (Northeastern Russia) (Andreev & Pevzner 2001, Solomina et al. 2008, Pendea et al. 2017). A multidisciplinary approach enables detailed reconstruction of past environmental conditions while providing an integrated perspective on vegetation-climate-geological process interactions and their long-term ecosystem-shaping dynamics. Situated between the Pacific Ocean and the Eurasian continent, coupled with its intense volcanic activity, the Kamchatka Peninsula represents a critical area for reconstructing vegetation and climatic changes in the Northern Pacific region (Jones & Solomina 2015, Brooks et al. 2015).

Paleoenvironmental research in the Kamchatka Peninsula began in the second half of the 20th century, with palynological

studies conducted on over 25 Late Quaternary sediment sections across the peninsula. Despite these efforts, several areas remain insufficiently studied or completely unexplored. Northern Kamchatka, characterized by harsh climatic conditions and relative inaccessibility, is one of the least understood regions in terms of paleoenvironmental history. It is represented by only four published paleoreconstructions based on peat and lake sediments, covering the Middle and Late Holocene (last 6 kyr). Additionally, data on Late Pleistocene vegetation are extremely scarce, limited to two paleorecords along the lower Kamchatka River (Pendea et al. 2017, Mukhametshina et al. 2022).

Consequently, the two main aims of this study are: (1) to reconstruct the Late Pleistocene and Holocene vegetation dynamics of northern Kamchatka using pollen analysis,

and (2) to synthesize the obtained results with previously published data to enhance insights into spatio-temporal changes in vegetation across the entire Kamchatka Peninsula.

## MATERIAL AND METHODS

### Study area

The study site is a shrub-sedge oligotrophic mire located along the bank of the Hadey stream – a right tributary of the Lomutskaya River (57.523556°N 161.260111°E, 223 m a.s.l.) (Fig. 1). According to the vegetation classification by Neshataeva (2011), the mire is located at the boundary between the Lower Kamchatka (birch–coniferous forest) district and the northeastern coastal district which is characterized by the predominance of dwarf shrub tundra communities with dwarf alder (*Alnus alnobetula* subsp. *fruticosa* (Rupr.) Raus) and Siberian dwarf pine (*Pinus pumila* (Pall.) Regel), as well as mires dominated by Siberian dwarf pine, shrubs, lichens, hypnum and sphagnum mosses (Neshataeva 2011). Following Neshataev & Neshataeva (2018), the study region is characterized by a moderately cold climate with a dry and cold summer. According to Kondratyuk (1974), the climate of the area is characterized by a harsh winter (-16 to -18°C in January) and a snow cover of up to 150 cm, a cool summer (11–12°C in July), and an average level of humidity (600–700 mm per year).

To collect peat samples, a geological shaft was dug to a depth of 200 cm in the southeastern relatively dry margin of the mire. The peat deposit was composed of alternating layers of peat and volcanic ash. The stratigraphy of the section was described in the field, and tephra layers were identified (Fig. 2). Both the radiocarbon dates obtained and the continuous tracking method for correlating tephra layers were employed for tephra identification. The correlation of the tephra layers was based on a profile from the northwest flank of Shiveluch Volcano (sections 1–6) (Pevzner 2010).

We performed radiocarbon dating on 11 peat samples at the Geological Institute RAS using the standard method (Pevzner 2015) on alkaline extracts from peat (Table 1). Peat samples with a thickness of 2 cm were used for dating. Using multiple dates from the same sample improves the precision in determining the formation time of the 2 cm peat layer. For calibration of radiocarbon dates and for the calculation of the combined age for each sample, the R\_combine function in the OxCal v.4.4.2 software was used (Bronk Ramsey 2009). To assess the sediment accumulation rate at the Hadey section, an age–depth model was developed using the rBacon package in the R environment (Blaauw & Christen 2011). All ages, except as specifically noted, are given in calibrated years.

To reconstruct vegetation dynamics, we performed pollen analysis of the same 11 peat samples used for radiocarbon dating, following the standard method (Grichuk 1940). Pollen grains were extracted using a heavy liquid HPS-W (heteropolyoxotungstates solution) with a density of 2.2 kg/m<sup>3</sup>. *Lycopodium* spores (Batchnr. 1031) were added as an exotic marker to determine the pollen concentration. Pollen percentages were calculated relative to the total pollen sum excluding Cyperaceae, while spore percentages were calculated relative to the sum of pollen and spores.

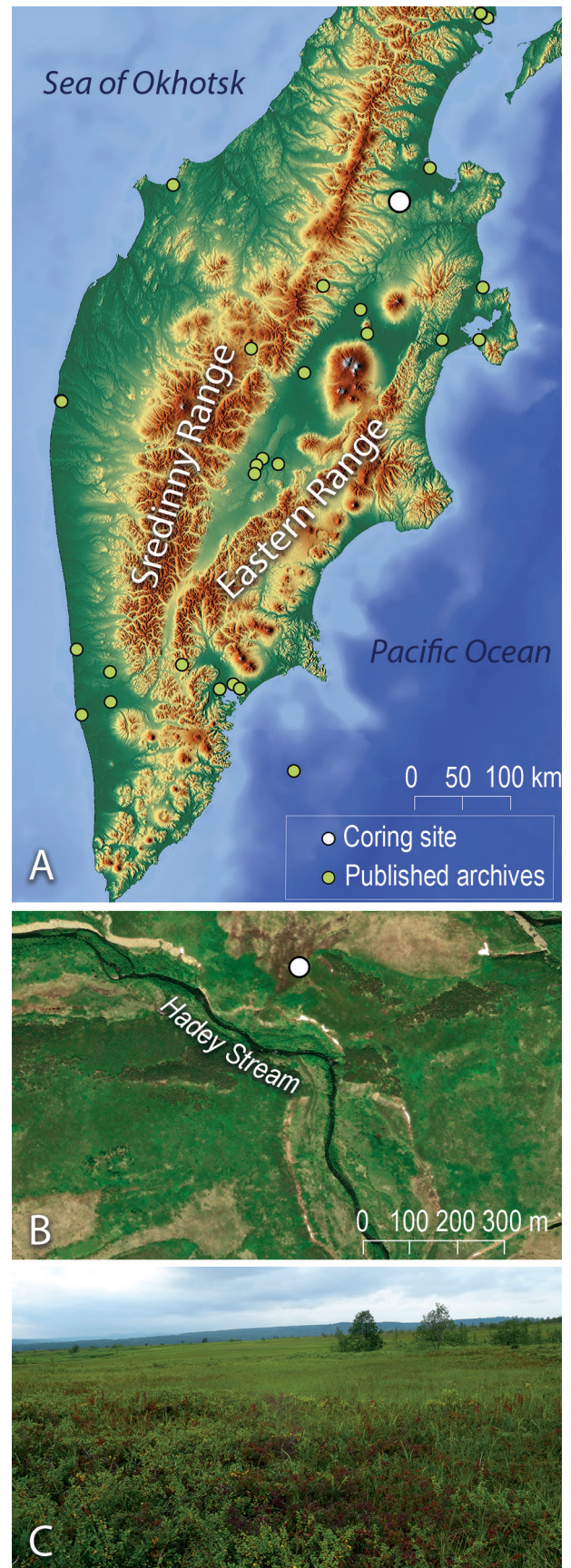


**Figure 1** Study area: a) Map of the study region with the location of the Hadey mire on the Kamchatka Peninsula (marked with a white dot), along with sites of published pollen-inferred paleoreconstructions; b) ESRI satellite image showing the location of the coring site; c) Photograph of the study mire, taken at the sampling site (photo by Maria Pevzner)

**Table 1.** Radiocarbon dates of the Hadey peat deposits.

№	GIN-	Fraction*	Age ( <sup>14</sup> C yr BP)	Calibrated dates, BP, median±σ	Combined calibrated dates, BP, median±σ	Calibrated dates, BP**																																																																																																			
1	16108	2	1330±30	1260±40	1290±30	1305–1265 (82.0) 1207–1177 (13.5)																																																																																																			
		1	1370±30	1290±30			2	16109	2	1620±30	1480±40	1520±50	1573–1413 (95.4)	1	1660±30	1550±60	3	16110	1	3030±30	3230±60	3240±51	3340–3286 (31.4) 3271–3166 (64.0)	2	3040±30	3250±55	4	16111	2	3490±30	3760±50	3780±45	3876–3811 (29.4) 3805–3700 (66.0)	1	3550±30	3850±60	5	16112	2	5030±30	5810±70	5820±50	5901–5745 (95.4)	1	5100±30	5800±50	6	16113	2	5880±30	6700±40	6760±40	6837–6819 (5.2) 6797–6674 (90.3)	1	5990±30	6830±50	7	16114	2	6770±30	7620±30	7650±25	7695–7604 (95.4)	1	6880±30	7710±40	8	16115	2	7850±30	8600±60	8720±90	8979–8829 (19.9) 8784–8629 (72.2) 8624–8601 (3.4)	1	7980±30	8860±90	9	16116	1	8830±30	9890±120	10130±90	10203–10116 (51.8) 10066–10006 (19.4) 9994–9916 (24.3)	2	9060±30	10220±20	10	16117	1	10460±60	12390±170	12390±170*** 12540±50	12655–12058 (95.4) 12664–12479 (95.4)	3	10520±60	12540±130	2	10530±30	12540±55	11	16118	2	10540±30	12540±60	12540±60
2	16109	2	1620±30	1480±40	1520±50	1573–1413 (95.4)																																																																																																			
		1	1660±30	1550±60			3	16110	1	3030±30	3230±60	3240±51	3340–3286 (31.4) 3271–3166 (64.0)	2	3040±30	3250±55	4	16111	2	3490±30	3760±50	3780±45	3876–3811 (29.4) 3805–3700 (66.0)	1	3550±30	3850±60	5	16112	2	5030±30	5810±70	5820±50	5901–5745 (95.4)	1	5100±30	5800±50	6	16113	2	5880±30	6700±40	6760±40	6837–6819 (5.2) 6797–6674 (90.3)	1	5990±30	6830±50	7	16114	2	6770±30	7620±30	7650±25	7695–7604 (95.4)	1	6880±30	7710±40	8	16115	2	7850±30	8600±60	8720±90	8979–8829 (19.9) 8784–8629 (72.2) 8624–8601 (3.4)	1	7980±30	8860±90	9	16116	1	8830±30	9890±120	10130±90	10203–10116 (51.8) 10066–10006 (19.4) 9994–9916 (24.3)	2	9060±30	10220±20	10	16117	1	10460±60	12390±170	12390±170*** 12540±50	12655–12058 (95.4) 12664–12479 (95.4)	3	10520±60	12540±130			2	10530±30	12540±55			11	16118	2	10540±30	12540±60	12540±60	12675–12578 (42.3) 12560–12480 (53.4)	1	10540±30	12540±60		
3	16110	1	3030±30	3230±60	3240±51	3340–3286 (31.4) 3271–3166 (64.0)																																																																																																			
		2	3040±30	3250±55			4	16111	2	3490±30	3760±50	3780±45	3876–3811 (29.4) 3805–3700 (66.0)	1	3550±30	3850±60	5	16112	2	5030±30	5810±70	5820±50	5901–5745 (95.4)	1	5100±30	5800±50	6	16113	2	5880±30	6700±40	6760±40	6837–6819 (5.2) 6797–6674 (90.3)	1	5990±30	6830±50	7	16114	2	6770±30	7620±30	7650±25	7695–7604 (95.4)	1	6880±30	7710±40	8	16115	2	7850±30	8600±60	8720±90	8979–8829 (19.9) 8784–8629 (72.2) 8624–8601 (3.4)	1	7980±30	8860±90	9	16116	1	8830±30	9890±120	10130±90	10203–10116 (51.8) 10066–10006 (19.4) 9994–9916 (24.3)	2	9060±30	10220±20	10	16117	1	10460±60	12390±170	12390±170*** 12540±50	12655–12058 (95.4) 12664–12479 (95.4)	3	10520±60	12540±130			2	10530±30	12540±55			11	16118	2	10540±30	12540±60	12540±60	12675–12578 (42.3) 12560–12480 (53.4)	1	10540±30	12540±60												
4	16111	2	3490±30	3760±50	3780±45	3876–3811 (29.4) 3805–3700 (66.0)																																																																																																			
		1	3550±30	3850±60			5	16112	2	5030±30	5810±70	5820±50	5901–5745 (95.4)	1	5100±30	5800±50	6	16113	2	5880±30	6700±40	6760±40	6837–6819 (5.2) 6797–6674 (90.3)	1	5990±30	6830±50	7	16114	2	6770±30	7620±30	7650±25	7695–7604 (95.4)	1	6880±30	7710±40	8	16115	2	7850±30	8600±60	8720±90	8979–8829 (19.9) 8784–8629 (72.2) 8624–8601 (3.4)	1	7980±30	8860±90	9	16116	1	8830±30	9890±120	10130±90	10203–10116 (51.8) 10066–10006 (19.4) 9994–9916 (24.3)	2	9060±30	10220±20	10	16117	1	10460±60	12390±170	12390±170*** 12540±50	12655–12058 (95.4) 12664–12479 (95.4)	3	10520±60	12540±130			2	10530±30	12540±55			11	16118	2	10540±30	12540±60	12540±60	12675–12578 (42.3) 12560–12480 (53.4)	1	10540±30	12540±60																						
5	16112	2	5030±30	5810±70	5820±50	5901–5745 (95.4)																																																																																																			
		1	5100±30	5800±50			6	16113	2	5880±30	6700±40	6760±40	6837–6819 (5.2) 6797–6674 (90.3)	1	5990±30	6830±50	7	16114	2	6770±30	7620±30	7650±25	7695–7604 (95.4)	1	6880±30	7710±40	8	16115	2	7850±30	8600±60	8720±90	8979–8829 (19.9) 8784–8629 (72.2) 8624–8601 (3.4)	1	7980±30	8860±90	9	16116	1	8830±30	9890±120	10130±90	10203–10116 (51.8) 10066–10006 (19.4) 9994–9916 (24.3)	2	9060±30	10220±20	10	16117	1	10460±60	12390±170	12390±170*** 12540±50	12655–12058 (95.4) 12664–12479 (95.4)	3	10520±60	12540±130			2	10530±30	12540±55			11	16118	2	10540±30	12540±60	12540±60	12675–12578 (42.3) 12560–12480 (53.4)	1	10540±30	12540±60																																
6	16113	2	5880±30	6700±40	6760±40	6837–6819 (5.2) 6797–6674 (90.3)																																																																																																			
		1	5990±30	6830±50			7	16114	2	6770±30	7620±30	7650±25	7695–7604 (95.4)	1	6880±30	7710±40	8	16115	2	7850±30	8600±60	8720±90	8979–8829 (19.9) 8784–8629 (72.2) 8624–8601 (3.4)	1	7980±30	8860±90	9	16116	1	8830±30	9890±120	10130±90	10203–10116 (51.8) 10066–10006 (19.4) 9994–9916 (24.3)	2	9060±30	10220±20	10	16117	1	10460±60	12390±170	12390±170*** 12540±50	12655–12058 (95.4) 12664–12479 (95.4)	3	10520±60	12540±130			2	10530±30	12540±55			11	16118	2	10540±30	12540±60	12540±60	12675–12578 (42.3) 12560–12480 (53.4)	1	10540±30	12540±60																																										
7	16114	2	6770±30	7620±30	7650±25	7695–7604 (95.4)																																																																																																			
		1	6880±30	7710±40			8	16115	2	7850±30	8600±60	8720±90	8979–8829 (19.9) 8784–8629 (72.2) 8624–8601 (3.4)	1	7980±30	8860±90	9	16116	1	8830±30	9890±120	10130±90	10203–10116 (51.8) 10066–10006 (19.4) 9994–9916 (24.3)	2	9060±30	10220±20	10	16117	1	10460±60	12390±170	12390±170*** 12540±50	12655–12058 (95.4) 12664–12479 (95.4)	3	10520±60	12540±130			2	10530±30	12540±55			11	16118	2	10540±30	12540±60	12540±60	12675–12578 (42.3) 12560–12480 (53.4)	1	10540±30	12540±60																																																				
8	16115	2	7850±30	8600±60	8720±90	8979–8829 (19.9) 8784–8629 (72.2) 8624–8601 (3.4)																																																																																																			
		1	7980±30	8860±90			9	16116	1	8830±30	9890±120	10130±90	10203–10116 (51.8) 10066–10006 (19.4) 9994–9916 (24.3)	2	9060±30	10220±20	10	16117	1	10460±60	12390±170	12390±170*** 12540±50	12655–12058 (95.4) 12664–12479 (95.4)	3	10520±60	12540±130			2	10530±30	12540±55			11	16118	2	10540±30	12540±60	12540±60	12675–12578 (42.3) 12560–12480 (53.4)	1	10540±30	12540±60																																																														
9	16116	1	8830±30	9890±120	10130±90	10203–10116 (51.8) 10066–10006 (19.4) 9994–9916 (24.3)																																																																																																			
		2	9060±30	10220±20			10	16117	1	10460±60	12390±170	12390±170*** 12540±50	12655–12058 (95.4) 12664–12479 (95.4)	3	10520±60	12540±130			2	10530±30	12540±55			11	16118	2	10540±30	12540±60	12540±60	12675–12578 (42.3) 12560–12480 (53.4)	1	10540±30	12540±60																																																																								
10	16117	1	10460±60	12390±170	12390±170*** 12540±50	12655–12058 (95.4) 12664–12479 (95.4)																																																																																																			
		3	10520±60	12540±130																																																																																																					
		2	10530±30	12540±55			11	16118	2	10540±30	12540±60	12540±60	12675–12578 (42.3) 12560–12480 (53.4)	1	10540±30	12540±60																																																																																									
11	16118	2	10540±30	12540±60	12540±60	12675–12578 (42.3) 12560–12480 (53.4)																																																																																																			
		1	10540±30	12540±60																																																																																																					

**Notes:** \* – Radiocarbon dating was conducted on peat samples, with three types of fractions analyzed: 1 – cold alkaline extract, 2 – hot extract from the residue of fraction 1, and 3 – plant detritus. \*\* – The most probable calibrated ages are reported, with the probability percentages for each interval shown in parentheses. \*\*\* – GIN-16117-1 date was not combined with GIN-16117-2,3 due to the large uncertainty associated with the cold alkaline extract result. BP refers to “before present”.

To compare the obtained results and conduct a spatio-temporal analysis, we used published data (Table 2). We selected only paleoecological reconstructions based on pollen analysis that included radiocarbon dating or reliable tephrochronology. Most of the referenced pollen records are from lake and peat deposits with a predominantly regional pollen and lack a strong local component. Therefore, tree pollen percentages in those records reflect regional vegetation dynamics. To ensure comparability with these datasets, we excluded Cyperaceae pollen from the basic pollen sum in our record, as sedge pollen is often overrepresented in local mire conditions. Changes in the proportion of birch pollen (*Betula ermanii* and *B. platyphylla*) and Siberian dwarf pine (*Pinus pumila*) pollen across the Kamchatka Peninsula were analyzed. For each site, we determined the age at which birch pollen exceeded 10 % and *Pinus pumila* pollen exceeded 5 % in the spectra. These threshold values were chosen based on the reproductive biology of the species and their pollen dispersal characteristics (Mukhametshina 2024).

## RESULTS

### Stratigraphy and chronology

A dense, viscous light-gray loam, enriched with small gravel, measuring 15 cm in thickness, lies at the base of the study section (Fig. 2). Above this loam is a peat deposit with a total thickness of 184 cm. The lowermost 7 cm of the peat consist of slightly loamy material, while the bottommost 2 cm display a pronounced admixture of loam, coarse sand, and fine gravel originating from the underlying strata. These basal 2 cm were not used for radiocarbon dating because peat-enriched loams usually show much younger ages (Pevzner 2015).

Thirteen tephra layers >0.5 cm thick and 2–3 additional layers (<0.5 cm) were identified within the peat deposit. Most of these are marker tephtras from distant volcanoes (>100 km) – Shiveluch, Khangar and Ksudach – with individual layer thicknesses not exceeding 4 cm. Additionally, tephra from nearby volcanoes is represented by deposits from the Kinenin maar (located 26 km from the sampling site) and the Ozernovsky lava flow (38 km from the sampling site). The tephra from the Ozernovsky flow (OZ) is found in the lower part of the section, consisting of two horizons: the lower ochreous sands from a phreatomagmatic explosion and the overlying black volcanic sands of a scoria cone. Together, they have a combined thickness of 25 cm.

The results of radiocarbon dating of the Hadey peat deposits are presented in Fig. 2 and Table 1. In total, 23 radiocarbon ages were obtained from 11 samples. For the construction of the age-depth model, 11 combined dates were used (Table 1). The date obtained from sample GIN-16117-1 has a relatively large confidence interval, a situation commonly encountered when processing poorly decomposed peat. Better preservation of plant remains is indicated by the date GIN-16117-3, which was obtained from plant detritus remaining after alkaline treatment of the sample (the only such case in the entire section). Apparently, the weak decomposition of the peat is due to its preservation beneath a thick OZ tephra layer. Since eutrophic peat containing sedge roots was used for determining the age of the lower part of the deposit, dates GIN-16117 and GIN-16118 may be rejuvenated (appearing younger than their true age). To more accurately determine the age of peatland initiation and the OZ eruption, we use the oldest calibrated ages derived from

**Table 2.** Published paleoenvironmental reconstructions that were used to create Figure 6.

№	Site name	References	Latitude	Longitude
1	Ust'-Khairuzovo Peatland	Dirksen et al, 2013 and references therein	57.10206	156.75579
2	Kirganik Tundra Peatland	Dirksen et al, 2013 and references therein	54.87029	158.82042
3	Cherny Yar Peatland	Dirksen et al, 2013 and references therein	56.22894	162.12357
4	Stolbovaya Peatland	Dirksen et al, 2013 and references therein	56.71845	162.82562
5	Uka Peatland	Dirksen et al, 2013 and references therein	57.78062	162.08374
6	Icha Peatland	Dirksen et al, 2013 and references therein	55.67565	155.66082
7	Lifebuoy Lake	Solovieva et al. 2015	59.10537	163.15718
8	Pechora Lake	Andren et al. 2015	59.29387	163.12995
9	Olive-Backed Lake	Self et al. 2015	56.20146	158.85881
10	Two-Yurts Lake	Hoff et al. 2015	56.81550	160.05304
11	Sokoch Lake	Dirksen et al. 2015	53.25266	157.75210
12	Utka Peatland	Klimaschewski et al. 2015	53.25081	156.85395
13	Krutoberegovo Peatland	Pendea et al. 2017	56.25000	162.70972
14	KamPlen	Mukhametshina et al. 2022	56.34923	160.65625
15	Kich Peatland	Mukhametshina et al. 2024	56.44075	160.9998
16	Kumroch Peatland	Unpublished data	56.55234	161.81799
17	Hadey Peatland	This study	57.52356	161.26011

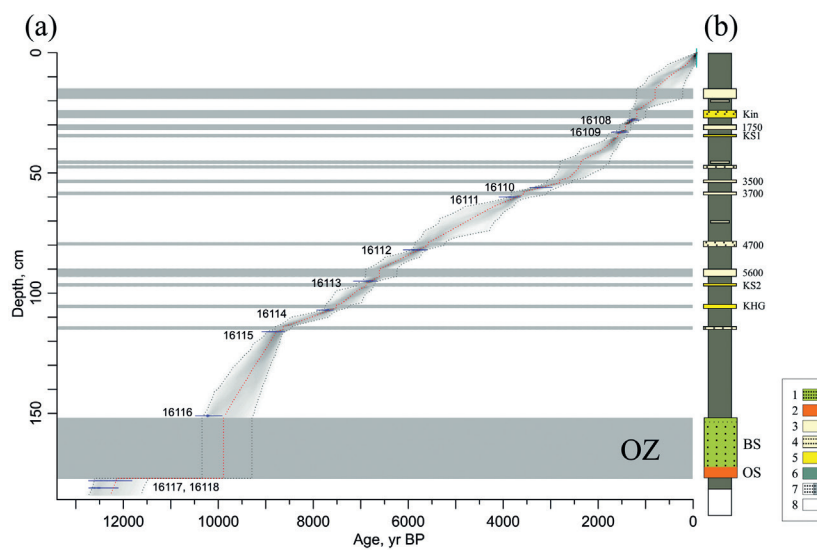


**Figure 2** The age-depth model (a) and stratigraphic scheme (b) of the Hadey peat deposit. The calibrated  $^{14}\text{C}$  dates are shown in blue, darker greys indicate more likely ages, grey dashed lines show 95% confidence intervals, the red dashed line shows the single 'best' model based on the mean age for each sampling depth and the grey horizontal line marks the ash layers. Legend: 1, 2 – tephra from the Ozernovsky lava flow (OZ): BS – black volcanic sands of a scoria cone; OS – ochreous sands from a phreatomagmatic explosion; 3, 4 – tephra from Shiveluch volcano (with rounded  $^{14}\text{C}$  ages): 3 – thin volcanic ash; 4 – granular volcanic sand; 5 – marker ash layers from distant volcanoes: Kin – Kinenin maar (~1.20 kyr), KS1 and KS2 – Ksudach (~1.65 and ~6.76 kyr), KHG – Khangar (~7.87 kyr) (eruption ages after Portnyagin et al. 2020); 6 – peat; 7 – sand; 8 – loam

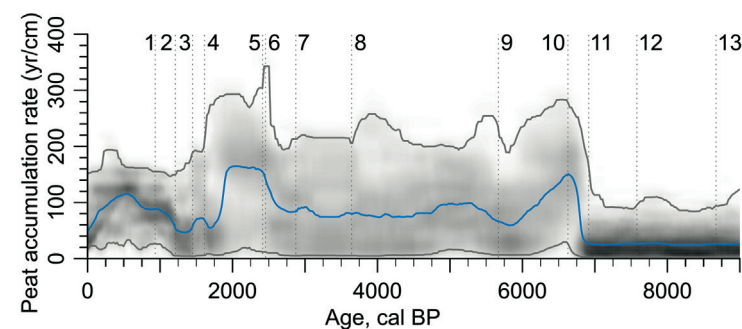


**Figure 3** The peat accumulation rate of the Hadey peat deposit. The blue line represents the mean value, while the gray shading shows the 95% probability interval. Darker areas correspond to higher probability values based on the age-depth model. Dashed vertical lines indicate tephra layers from volcanoes: 1, 3, 5–10, 13 – Shiveluch; 2 – Kinenin maar; 4, 11 – Ksudach; 12 – Khangar

the age-depth model (Fig. 2). According to this model, peat accumulation at the studied mire began about 12.72 kyr BP, and the OZ eruption occurred between 12.65 and 12.6 kyr BP.

The peat accumulation rate (PAR) data were obtained using the age-depth model for the past 9 kyr (Fig. 3). Three distinct phases of reduced PAR were identified: 7–6 kyr BP, 2.5–1.8 kyr BP, 1.25–0.25 kyr BP. Maximum peat accumulation rates were observed during the intervals of 9.0–6.9 kyr BP and 1.25–1.75 kyr BP.

### Pollen analysis

Eleven peat samples were used for pollen analysis. Each pollen spectrum is numbered to correspond with the associated radiocarbon-dated sample. The resulting pollen diagram is presented in Fig. 4.

Samples 11 and 10 from the base of the peat deposit (12.6–12.4 kyr BP), exhibit similar pollen spectrum compositions. The spectra are dominated by pollen of *Alnus alnobetula* subsp. *fruticosa*, *Betula nana*, Poaceae, Cyperaceae, *Artemisia*, and *Thalictrum*. Sporadic occurrences of other herbaceous taxa (Caryophyllaceae, *Polemonium*, Scrophulariaceae, and Chenopodiaceae) are also detected. Among spores, Polypodiaceae and *Equisetum* are predominant, with occasional appearances of *Lycopodium* and *Sphagnum* spores.

Samples 9–5 (10.0–5.8 kyr BP) represent a distinct group. Although shrub pollen remains dominant, these spectra show a higher proportion of *Thalictrum*, Rosaceae, and Poaceae, alongside a decline in *Artemisia*. Meadow taxa, including Asteraceae, Fabaceae, Lamiaceae, and Apiaceae, become more prominent. Among spores, Polypodiaceae are predominant in samples 8 and 9, while both Polypodiaceae and *Lycopodium* dominate in

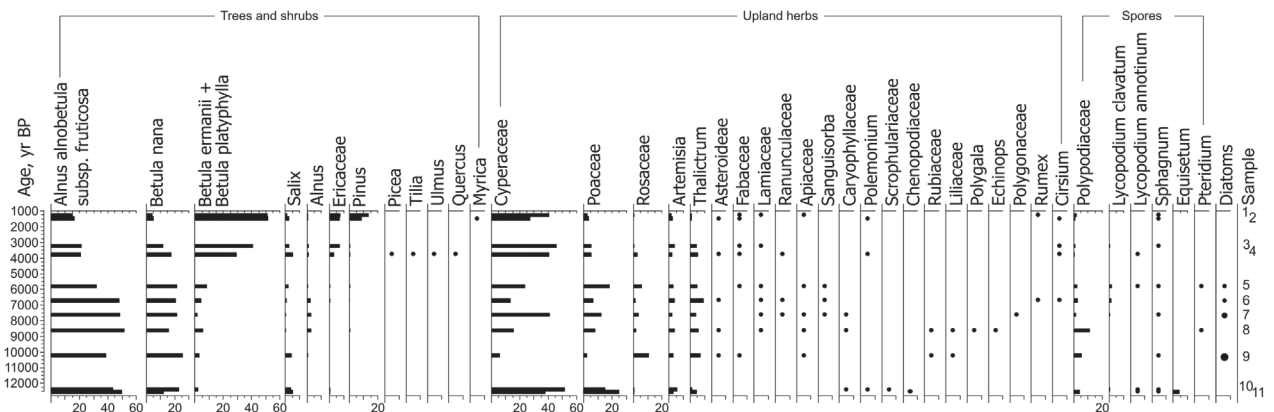


**Figure 4** Pollen diagram of the Hadey peat deposits. Pollen percentages are calculated based on the total number of pollen grains excluding Cyperaceae, while spore percentages are calculated based on the sum of pollen grains and spores

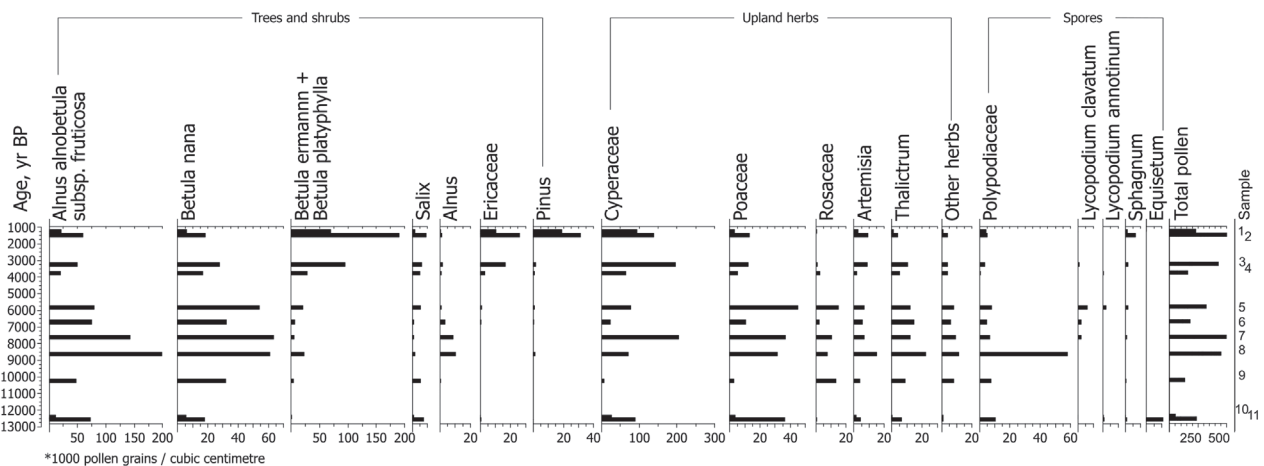


**Figure 5** Pollen concentration diagram of the Hadey peat deposits (pollen grains per  $1\text{ cm}^3 \times 1000$ )

samples 7–5. A substantial quantity of diatom is also present throughout samples 9–5.

Samples 3 and 4 (3.8–3.2 kyr BP) are characterized by the dominance of tree birch pollen (*Betula ermanii* + *B. platyphylla*). There is also an increased proportion of Cyperaceae, Ericaceae, and *Salix* pollen. Occasional grains of broadleaf trees (*Tilia*, *Ulmus*, *Quercus*) and *Picea* are present in sample 4. Samples 1 and 2 (1.5–1.2 kyr BP) are distinguished by the highest proportions of *Betula ermanii* + *B. platyphylla*, *Pinus pumila*, Ericaceae, and Cyperaceae pollen.

Pollen concentration analysis in the spectra (Fig. 5) showed that spectrum 11 from the base of the section, dated to 12.7 kyr BP, is characterized by a lower concentration of arboreal pollen compared to Holocene spectra. In sample 10 (located beneath the OZ tephra layer), the concentration value is 3–5 times lower than in the preceding sample, although the percentage composition of the pollen spectra for these samples is similar (Fig. 3). At the boundary between the Late and Middle Holocene (8.5–8.2 kyr BP), a general increase in pollen concentration was recorded. Significant changes in pollen concentration were also observed between samples 1 and 2. While the proportions of major pollen types remained consistent, the pollen concentration in sample 1 was 2–2.5 times lower than in sample 2.

## DISCUSSION

### Peatland initiation and peat accumulation dynamics

Radiocarbon dating showed peat deposition at the Hadey site began approximately 12.7 kyr BP and was associated with the Bølling-Allerød–Younger Dryas transition. It predates the peatland initiation ages of most mires studied on the Kamchatka Peninsula (Zakharikhina 2014). Peat accumulation is influenced by both the rate of sediment accumulation and decomposition, which are primarily determined by moisture conditions (Weckström et al. 2010, Lavoie et al. 2013, Quik 2023). A similar or even older age of peat initiation has been determined for two mires in Kamchatka – the Nachiki site (Pevzner 2015) and the Krutoberegovo site (Pendea et al. 2017), as well as for neighboring regions of the Russian Far East – Chukotka (Lozhkin et al. 2011) and the Kuril Islands (Razjigaeva et al. 2011). It suggests that the Kamchatka Peninsula was characterized by sufficient moisture levels during the last two millennia of the Late Pleistocene.

OZ tephra deposition (12.6 kyr BP) interrupted peat accumulation for approximately 2.5 kyr, with sedimentation resuming around 10.1 kyr BP. The dynamics of the peat accumulation rate (PAR) during the Holocene (Fig. 3) indicate that tephra deposition did not have a significant long-term

impact on peat accumulation. However, the Ksudach 2 tephra may have contributed to a temporary reduction in peat accumulation rates. Other tephra layers did not noticeably affect the PAR. Volcanic events can locally and temporarily influence peat accumulation, but overall PAR dynamics are likely driven primarily by climatic conditions. Periods of reduced PAR correspond to drier and warmer climatic intervals on the peninsula, notably at 6–6.5 and 1.9–2.3 kyr BP (Dirksen et al. 2013, Brooks et al. 2015).

## Vegetation dynamics

Pollen analysis of the Hadey peat deposits enables the reconstruction of vegetation dynamics in northern Kamchatka during the Late Pleistocene and Holocene. In the pollen spectra corresponding to the Late Pleistocene (12.6–12.7 kyr BP), shrubs pollen (*Alnus alnobetula* subsp. *fruticosa*, *Betula nana*) and grasses pollen predominates, indicating the prevalence of alder shrub communities and meadow-tundra ecosystems as well as relatively cold climatic conditions. These findings are consistent with previous studies from the Kamchatka Peninsula (Meyer et al. 2017, Pendea et al. 2017) and with vegetation reconstructions from western Beringia (Anderson et al. 2015).

During the Early Holocene (11.7–8.2 kyr BP), no significant changes occurred in the composition of plant communities. However, an increase in overall pollen con-

centration is observed, which indirectly indicates a rise in mean annual temperatures (Abraham et al. 2021). Alder shrub communities continued to dominate the study area. Additionally, an increase in the local wetness of the peatland is recorded (evidenced by a higher proportion of hydrophilous taxa, the presence of diatom algae, and a high rate of peat accumulation).

Approximately 6 kyr BP, shrub communities began to decline in their contribution to the regional vegetation cover. This shift corresponds with mid-Holocene climatic warming, as evidenced in numerous peat and lake sediment cores across the Kamchatka Peninsula (Table 2). The widespread establishment of birch forests in northeastern Kamchatka is attributed to the late Holocene, within the last 4.2 kyr BP. Previous research indicates that birch forests began to expand across the peninsula as early as 10 kyr BP, originating from southeastern and central part of the peninsula (Dirksen et al. 2013). Birch forests consisting mainly of *Betula ermanii* or *B. platyphylla* spread along the Kamchatka River valley and adjacent mountain slopes, reached its lower basin approximately 7 kyr BP (Andreev & Pevzner 2001) and the Pacific coastline approximately 6 kyr BP (Pendea et al. 2017). According to pollen data from the Hadey mire and other reconstructions from northeastern Kamchatka (Dirksen et al. 2013), birch forests did not become the dominant vegetation in the study area until around 4 kyr BP. In contrast, farther north, near the settlement of Ossora, birch pollen has remained at background levels with minimal variation over the past 6 kyr, suggesting that birch forests played a minor role in the vegetation cover of that region (Andren et al. 2015, Solovieva et al. 2015).

Pollen records from the Hadey mire reveal that Siberian dwarf pine (*Pinus pumila*) has become progressively more prominent in vegetation of the study area over the past ~2 kyr BP. However, according to Hammarlund et al. (2015), the initial occurrence of *P. pumila* pollen in northern Kamchatka (near the settlement of Ossora) dates to approximately 6.5–5.5 kyr BP, with a marked increase approximately 4 kyr BP. In the Sredinny Range (Anavgay area), lake sediment records reveal the early presence of *P. pumila* pollen around 5–4 kyr BP, which is 2–3 millennia earlier than in the Hadey peat section (Khomentovskiy et al. 1995, Hammarlund et al. 2015). Along the Pacific coast, *Pinus pumila* pollen in peat sediment appears much later, 1000 yr BP, as recorded at the Uka site on the coast of the Karaginsky Gulf (Dirksen et al. 2013). In contrast, sediment profiles near the mouth of the Kamchatka River (Dirksen et al. 2013, Pendea et al. 2017) and in northeastern part of

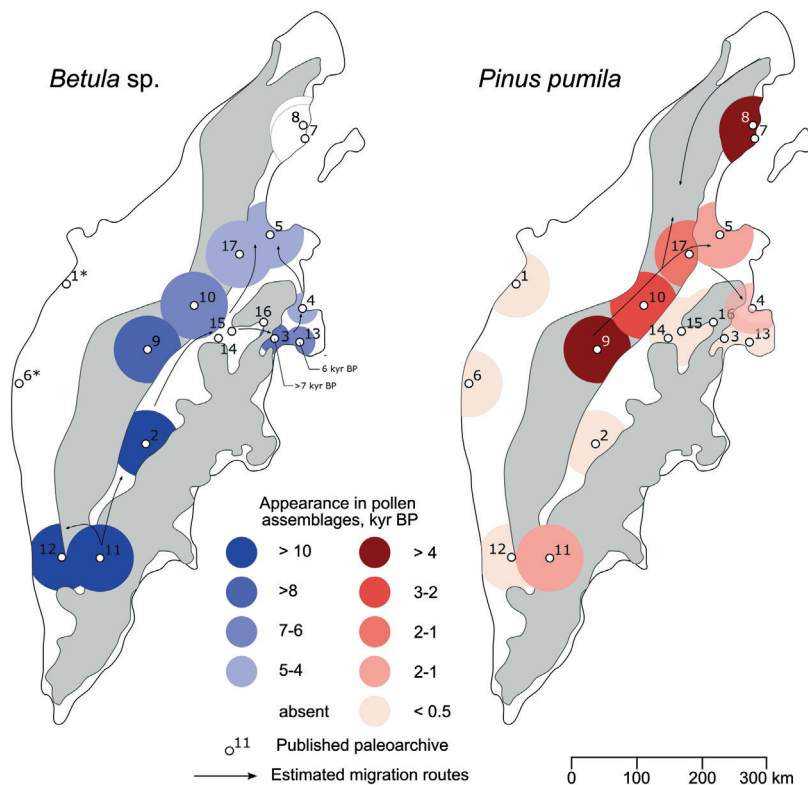


**Figure 6** Schematic models of the expansion dynamics of birch forests (*Betula ermanii* and *B. platyphylla*) and Siberian dwarf pine (*Pinus pumila*) communities across the Kamchatka Peninsula. The threshold for birch pollen is set at 10 %, reflecting its high dispersal ability, while for Siberian dwarf pine pollen it is set at 5 %. Color intensity of circles indicates the chronological appearance of pollen based on published paleoenvironmental reconstructions (see details in Table 2). The Hadey mire is marked by point 17

the Hadey mire reveal that Siberian dwarf pine (*Pinus pumila*) has become progressively more prominent in vegetation of the study area over the past ~2 kyr BP. However, according to Hammarlund et al. (2015), the initial occurrence of *P. pumila* pollen in northern Kamchatka (near the settlement of Ossora) dates to approximately 6.5–5.5 kyr BP, with a marked increase approximately 4 kyr BP. In the Sredinny Range (Anavgay area), lake sediment records reveal the early presence of *P. pumila* pollen around 5–4 kyr BP, which is 2–3 millennia earlier than in the Hadey peat section (Khomentovskiy et al. 1995, Hammarlund et al. 2015). Along the Pacific coast, *Pinus pumila* pollen in peat sediment appears much later, 1000 yr BP, as recorded at the Uka site on the coast of the Karaginsky Gulf (Dirksen et al. 2013). In contrast, sediment profiles near the mouth of the Kamchatka River (Dirksen et al. 2013, Pendea et al. 2017) and in northeastern part of

the peninsula (Andreev & Pevzner 2001, Mukhametshina et al. 2024) show only a minor proportion of *P. pumila* pollen, with no significant presence detected until recent times.

The pollen data obtained from the Hadey mire peat sequences contribute to a more refined understanding of the expansion dynamics of birch forests and the distribution patterns of Siberian dwarf pine communities across the Kamchatka Peninsula. A synthesis of these results is presented in Figure 6.

Geographically, the Hadey peatland lies among previously studied sites, supporting the hypothesis that *P. pumila* expansion on the Kamchatka Peninsula originated from two primary centers (the Sredinny Range and the Koryak Mountains). Analogous Siberian dwarf pine refugia have previously been studied in western Beringia (Khomentovskiy et al. 1995, Kremenetski et al. 1998, Anderson et al. 2010). Local populations of Siberian dwarf pine presumably persisted in the higher elevations of the Sredinny Range throughout the post-glacial period and the Early Holocene (Khomentovskiy et al. 1995). During subsequent Neoglacial cooling, these populations began to expand across the Kamchatka Peninsula (Hammarlund et al. 2015). A similar expansion occurred farther north, near the settlement of Ossora, where Siberian dwarf pine communities spread southward from the continental Koryak Mountains.

## CONCLUSION

This study reconstructs vegetation dynamics in northern Kamchatka during the Late Pleistocene–Holocene based on a comprehensive analysis of peat deposits. Pollen analysis, tephrostratigraphy, and radiocarbon dating significantly contribute to understanding spatiotemporal vegetation changes in this previously underexplored region. Peat accumulation at the study site commenced approximately 12.7 kyr BP, indicating adequate moisture availability during the terminal Pleistocene. Accumulation persisted throughout the Holocene, with the exception of an interruption between 12.5 and 10.1 kyr BP, caused by the deposition of the Ozernovskiy Flow tephra. During the Late Pleistocene, tundra and shrub communities dominated, reflecting the cold climatic conditions of the late-glacial period.

Around 6 kyr BP, coinciding with the Holocene Climatic Optimum, tree birch (*Betula ermanii* and *B. platyphylla*) established within the vegetation cover, reaching its maximum distribution approximately 4 kyr BP. Siberian dwarf pine (*Pinus pumila*) pollen appeared about 2 kyr BP, marking the initial spread of pine shrub communities in the region. A comprehensive spatiotemporal analysis, integrating both new and previously published data, enabled the reconstruction of the expansion dynamics of birch forests and dwarf pine communities across the Kamchatka Peninsula. The dispersal of birch forests followed a south-to-north trajectory, whereas the expansion of *Pinus pumila* occurred from two primary centers: the central part of the Sredinny Range and the Koryak Mountains.

## ACKNOWLEDGEMENTS

The authors express their sincere gratitude to Maria Nosova for providing exotic marker tablets. We also thank

L.A. Balibalova for her valuable assistance during fieldwork, and Ekaterina Ershova for helpful discussions and insightful comments on the manuscript. The reported study was funded by the Russian Science Foundation 24-14-00065 (pollen analysis). Radiocarbon dating was carried out within the framework of State Assignment No. FMMG-2022-0002.

**Author contribution:** VEP and MMP planned the research; MMP, TDK, AVP conducted the field sampling; VEP and DMN performed the pollen analyses; MMP, TDK, RIN conducted radiocarbon dating and tephrochronological analyses; VEP designed the visualization with support of MMP; VEP and MMP wrote the text, while all authors critically revised the manuscript and approved the final and revised version.

## LITERATURE CITED

- Abraham, V., S. Hicks, H. Svobodová-Svitavská, E. Bozilova, S. Panajiotidis, M. Filipova-Marinova, C.E. Jensen, S. Tonkov, I.A. Pidek, ... & T. Giesecke 2021. Patterns in recent and Holocene pollen accumulation rates across Europe – the Pollen Monitoring Programme Database as a tool for vegetation reconstruction. *Biogeosciences* 18(15):4511–4534.
- Anderson, P.M., A.V. Lozhkin, T.B. Solomatkina & T.A. Brown 2010. Paleoclimatic implications of glacial and postglacial refugia for *Pinus pumila* in western Beringia. *Quaternary Research* 73(2):269–276.
- Anderson, P.M. & A.V. Lozhkin 2015. Late Quaternary vegetation of Chukotka (Northeast Russia), implications for Glacial and Holocene environments of Beringia. *Quaternary Science Reviews* 107:112–128.
- Andreev, A.A. & M.M. Pevzner 2001. The vegetation history of the lower reaches of the Kamchatka River over the last 6000 years. *Botanicheskii Zhurnal* 86:39–45 (in Russian) [Андреев А.А., Певзнер М.М. 2001. История растительности низовой реки Камчатки за последние 6000 лет // Ботанический журнал. Т. 86, № 5. С. 39–45].
- Andrén, E., A. Klimaschewski, A.E. Self, N. St. Amour, A.A. Andreev, K.D. Bennett, D.J. Conley, T.W.D. Edwards, N. Solovieva & D. Hammarlund 2015. Holocene climate and environmental change in north-eastern Kamchatka (Russian Far East), inferred from a multi-proxy study of lake sediments. *Global and Planetary Change* 134:41–54.
- Blaauw, M. & J.A. Christen 2011. Flexible paleoclimate age-depth models using an autoregressive gamma process. *Bayesian Analysis* 6(3):618.
- Brooks, S.J., B. Diekmann, V.J. Jones & D. Hammarlund 2015. Holocene environmental change in Kamchatka: A synopsis. *Global and Planetary Change* 134:166–174.
- Dirksen, V., O. Dirksen & B. Diekmann 2013. Holocene vegetation dynamics and climate change in Kamchatka Peninsula, Russian Far East. *Review of Palaeobotany and Palynology* 190:48–65.
- Dirksen, V., O. Dirksen, C. van den Bogaard & B. Diekmann 2015. Holocene pollen record from Lake Sokoch, interior Kamchatka (Russia), and its paleobotanical and paleoclimatic interpretation. *Global and Planetary Change* 134:129–141.
- Hammarlund, D., A. Klimaschewski, N.A. St. Amour, E. Andrén, A.E. Self, N. Solovieva, A.A. Andreev, L. Barnekow & T.W.D. Edwards 2015. Late Holocene expansion of Siberian dwarf pine (*Pinus pumila*) in Kamchatka in response to increased snow cover as inferred from lacustrine oxygen-isotope records. *Global and Planetary Change* 134:91–100.

- Hoff, U., B.K. Biskaborn, V.G. Dirksen, O. Dirksen, G. Kuhn, H. Meyer, L. Nazarova, A. Roth & B. Diekmann 2015. Holocene environment of Central Kamchatka, Russia: Implications from a multi-proxy record of Two-Yurts Lake. *Global and Planetary Change* 134:101–117.
- Jones, V. & O. Solomina 2015. The geography of Kamchatka. *Global and Planetary Change* 134:3–9.
- Khomentovsky, P.A. 2004. *Ecology of Siberian dwarf pine Pinus pumila* (Pallas) Regel in Kamchatka. CRC Press, Boca Raton, 244 pp.
- Klimaschewski, A., L. Barnekow, K.D. Bennett, A.A. Andreev, E. Andrén, A.A. Bobrov & D. Hammarlund 2015. Holocene environmental changes in southern Kamchatka, Far Eastern Russia, inferred from a pollen and testate amoebae peat succession record. *Global and Planetary Change* 134:142–154.
- Kondratyuk, V.I. 1974. *Climate of Kamchatka*. Gidrometeoizdat, Moscow, 202 pp. (in Russian). [Кондратьев В.И. 1974. Климат Камчатки. Москва: Гидрометеоздат. 202 с.]
- Kremetski, C.V., K.-L. Liu & G.M. MacDonald. 2000. The Late Quaternary dynamics of pines in Northern Asia. In: *Ecology and biogeography of Pinus* (D.M. Richardson, ed.), pp. 95–106, Cambridge University Press, Cambridge.
- Lavoie, M., S. Pellerin & M. Larocque 2013. Examining the role of allogenic and autogenic factors in the long-term dynamics of a temperate headwater peatland (southern Québec, Canada). *Palaeogeography, Palaeoclimatology, Palaeoecology* 386:336–348.
- Lozhkin, A.V., P.M. Anderson & L.N. Vazhenina 2011. Younger Dryas and Early Holocene peats from northern Far East Russia. *Quaternary International* 237(1–2):54–64.
- Meyer, V., J. Hefter, G. Lohmann, L. Max, R. Tiedemann & G. Mollenhauer 2017. Summer temperature evolution on the Kamchatka Peninsula, Russian Far East, during the past 20000 years. *Climate of the Past* 13:359–377.
- Mukhametshina, E.O., E.A. Zelenin & I.F. Pendea 2022. Reconstruction of Late Glacial conditions of exogenic landscape formation of Central Kamchatka: Data on spore-pollen analysis. *Doklady Earth Sciences* 506(S1):S33–S41.
- Mukhametshina, E.O. 2024. Subfossil spore-pollen spectra of mountainous areas: the case of the Kamchatka Peninsula. *Geosistemy Perekhodnykh Zon* 8(2):127–141 (in Russian with English abstract). [Мухаметшина Е.О. 2024. Субфоссиальные спорово-пыльцевые спектры горных территорий на примере полуострова Камчатка // Геосистемы переходных зон. Т. 8, № 2, С. 127–141].
- Mukhametshina, E.O., M.D. Shchekleina & A.L. Zakharov 2024. Vegetation and climate changes in the north of the Central Kamchatka Depression in the Late Holocene. *Geomorfologiya i Paleogeografiya* 55(4):177–191 (in Russian with English abstract) [Мухаметшина Е.О., Шчеклеина М.Д., Захаров А.Л. 2024. Изменения растительности и климата севера Центральной Камчатской депрессии в позднем голоцене // Геоморфология и палеогеография. Т. 55, № 4. С. 177–191].
- Neshataeva, V.Yu. 2011. The plant cover of the Kamchatka Peninsula and its geobotanical subdivision. *Trudy Karelskogo Nauchnogo Tsentra RAN* 1:3–22 (in Russian with English abstract) [Нешатаева В.Ю. 2011. Растительный покров полуострова Камчатка и его геоботаническое районирование // Труды Карельского научного центра РАН. № 1. С. 3–22].
- Neshataeva, V. Yu. & V. Yu. Neshataev. 2018. Botanical and geographical features of the mires of the Kamchatka Region. In: *Vegetation of mires: current problems of classification, mapping, use and conservation* (N.A. Zelenkevich et al., eds), pp. 93–97, Kolodgrad, Minsk (in Russian). [Нешатаева В.Ю., Нешатаев В.Ю. 2018. Ботанико-географические особенности болот Камчатского края // Растительность болот: современные проблемы классификации, картографирования, использования и охраны: материалы V Международного научного семинара (16–20 сентября 2024 г.) / под ред. Н.А. Зеленкевича и др. Минск: Колорград. С. 93–97].
- Pendea, I.F., V. Ponomareva, J. Bourgeois, E.B.W. Zubrow, M. Portnyagin, I. Ponkratova, H. Harmsen & G. Korosec 2017. Late Glacial to Holocene paleoenvironmental change on the northwestern Pacific seaboard, Kamchatka Peninsula (Russia). *Quaternary Science Reviews* 157:14–28.
- Pevzner, M.M. 2010. The northern boundary of volcanic activity of Kamchatka in the Holocene. *Vestnik KRAUNC. Nauki o Zemle* 15(1):117–144 (in Russian with English abstract) [Певзнер М.М. 2010. Северная граница вулканической активности Камчатки в голоцене // Вестник КРАУНЦ. Науки о земле. Т. 15, № 1. С. 117–144].
- Pevzner, M.M. 2015. *Holocene volcanism of the Sredinny Range of Kamchatka*. GEOS, Moscow, 252 pp. (in Russian). [Певзнер М.М. 2015. Голоценовый вулканизм Срединного хребта Камчатки. Москва: ГЕОС. 252 с.]
- Portnyagin, M.V., V.V. Ponomareva, E.A. Zelenin, L.I. Bazanova, M.M. Pevzner, A.A. Plechova, A.N. Rogozin & D. Garbe-Schönberg 2020. TephraKam: geochemical database of glass compositions in tephra and welded tuffs from the Kamchatka volcanic arc (northwestern Pacific). *Earth System Science Data* 12(1):469–486.
- Quik, C. 2023. *Peatland initiation through time and space. Doctorate dissertation*. Wageningen University, Wageningen, Netherlands.
- Razjigaeva, N.G., L.A. Ganzey, K.A. Arslanov, T.A. Grebennikova, N.I. Belyanina & L.M. Mokhova 2011. Paleoenvironments of Kuril Islands in Late Pleistocene–Holocene: Climatic changes and volcanic eruption effects. *Quaternary International* 237(1–2):4–14.
- Self, A.E., A. Klimaschewski, N. Solovieva, V.J. Jones, E. Andrén, A.A. Andreev, D. Hammarlund & S.J. Brooks 2015. The relative influences of climate and volcanic activity on Holocene lake development inferred from a mountain lake in central Kamchatka. *Global and Planetary Change* 134:67–81.
- Solomina, O., I. Pavlova, A. Curtis, G. Jacoby, V. Ponomareva, M. Pevzner & M. Pevzner 2008. Constraining recent Shiveluch volcano eruptions (Kamchatka, Russia) by means of dendrochronology. *Natural Hazards and Earth System Sciences* 8(5):1083–1097.
- Solovieva, N., A. Klimaschewski, A.E. Self, V.J. Jones, E. Andrén, A.A. Andreev, D. Hammarlund, et al. 2015. The Holocene environmental history of a small coastal lake on the north-eastern Kamchatka Peninsula. *Global and Planetary Change* 134:55–66.
- Weckström, J., H. Seppä & A. Korhola 2010. Climatic influence on peatland formation and lateral expansion in sub-arctic Fennoscandia. *Boreas* 39(4):761–769.
- Zakharikhina, L.V. 2014. The rate of peat accumulation in the Holocene in Kamchatka. *Eurasian Soil Science* 47(6):556–561.